Applied Mathematics and Mechanics
(English Edition, Vol.8, No.3, Mar. 1987)

Published by SUT,
Shanghai, China

THE NUMERICAL SOLUTION OF THE UNSTEADY NATURAL CONVECTION FLOW IN A SQUARE CAVITY AT HIGH RAYLEIGH NUMBER USING SADI METHOD

Wang Pu (王 璞)
(*Lanzhou University, Lanzhou,*)
R. Kahawita
(*Ecole Polytechnique de Montreal, Canada*)

(Received Feb. 20, 1986 Communicated by Yeh Kai-yuan)

Abstract

The unsteady natural convection flow in a square cavity at high Rayleigh number $Ra=10^7$ and 2×10^7 has been computed using cubic spline integration. The required solutions to the two dimensional Navier-Stokes and energy equations have been obtained using two alternate numerical formulations on non-uniform grids. The main features of the transient flow have been briefly discussed. The results obtained by using the present method are in good agreement with the theoretical predictions[1,2]. The steady state results have been compared with accurate solutions presented recently for $Ra=10^7$.

I. Introduction

Cubic spline technique in the numerical integration of partial differential equations are today finding increased applications after the pioneering work of Rubin and Graves[3] and Rubin and Khosla[4]. The authors[5-7] extended the development of [3,4] and indicated the procedure for the reduction of the 3×3 matrices obtained with the previous formulation into a scalar system containing either the function values at the grid points, the first derivatives or the second derivatives[8].

Convection in cavities is an area of study with applications in a number of various domains. The majority of prior work on cavity convection has been concerned with steady-state situations[9-11]. Yet in many of the fields of application, the convective flows may be in a transient or unsteady state. Recognizing this fact, some of the recent work in the field has focused on the nature of the flow in the transient regime and the manner in which this flow evolves into the final steady state. The numerical results of unsteady natural convection flow in the above works have been obtained for $Ra=10^6$. For the value of $Ra=10^7$, the numerical transient solution seems to have been reported in the literature.

This paper reports on the results of an investigation undertaken to assess the efficiency of the technique in the solution of unsteady natural convection in a square cavity at $Ra=10^7$ and $Ra=2\times10^7$. The SADI (Spline Alternating Direction Implicit) procedure is used for solving the problem. Computations have been performed for Prandtl number $Pr=0.71$ and $Pr=2.7$. The main features of transient flow predicted by a scale analysis are briefly presented. The steady state results are in good agreement with accurate solutions presented recently for $\mathrm{Ra}=10^7$.

The results obtained are encouraging and make known that the cubic spline technique is an efficient method for solving the problem of the unsteady natural convection flow at high Rayleigh number, and justify further research in the field.

II. Mathematical Formulation

The geometry of the problem under consideration is indicated in Fig. 1. The aspect ratio of the half cavity is denoted by $E=l/H$. The Navier Stokes equations may be simplified and expressed as:

Continuity

$$\frac{\partial u}{\partial x}+\frac{\partial v}{\partial y}=0 \tag{2.1}$$

Momentum

$$\rho_0\left(\frac{\partial u}{\partial t}+u\frac{\partial u}{\partial x}+v\frac{\partial u}{\partial y}\right)=-\frac{\partial P}{\partial x}+\nu\nabla^2 u \tag{2.2}$$

$$\rho_0\left(\frac{\partial v}{\partial t}+u\frac{\partial v}{\partial x}+v\frac{\partial v}{\partial y}\right)=-\frac{\partial P}{\partial y}+\nu\nabla^2 u -g\rho_0[1-\beta(T-T_0)] \tag{2.3}$$

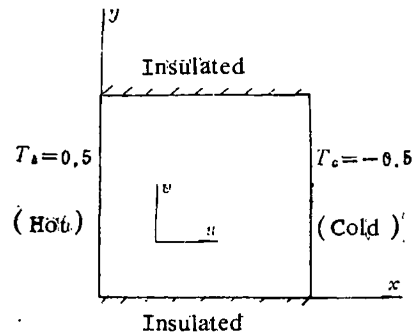

Fig. 1 Definition sketch of natural convection problem

Energy

$$\frac{\partial T}{\partial t}+u\frac{\partial T}{\partial x}+v\frac{\partial T}{\partial y}=a\nabla^2 T \tag{2.4}$$

where ∇^2 is the Laplacian operator, β is the bulk expansion coefficient, ν the viscosity coefficient, a the thermal diffusivity and ρ_0 is the density at the reference temperature T_0.

After elimination of the pressure between Eqs. (2.2) and (2.3), the use of the continuity equation (2.1) coupled with the vorticity expression, results in the following system of equations, where all the variables have been made dimensionless:

$$\nabla^2\psi=-\Omega \tag{2.5}$$

$$\frac{\partial\Omega}{\partial\tau}+\psi_Y\frac{\partial\Omega}{\partial X}-\psi_X\frac{\partial\Omega}{\partial Y}=\mathrm{Pr}\nabla^2\Omega+\mathrm{Pr}\cdot\mathrm{Ra}\frac{\partial\theta}{\partial X} \tag{2.6}$$

$$\frac{\partial\theta}{\partial\tau}\psi_Y\frac{\partial\theta}{\partial X}-\psi_X\frac{\partial\theta}{\partial Y}=\nabla^2\theta \tag{2.7}$$

where ψ is the stream function, $U=\frac{\partial\psi}{\partial Y}\equiv\psi_Y,\quad V=-\frac{\partial\psi}{\partial X}\equiv-\psi_X$;

with Ω is the vorticity $=-\left(\frac{\partial U}{\partial X}-\frac{\partial V}{\partial X}\right)$,

$$\tau=ta/L^2,\quad U=uL/a,\quad V=vL/a,\quad \theta=(T-T_0)/(T_h-T_c),\quad X=x/L,\quad Y=y/L$$

P_r = Prandtl Number Ra = Rayleigh Number.

Boundary conditions

The specified boundary conditions of the problem are:

at $X=0,\ \psi=\psi_X=0,\ \Omega=-\psi_{XX},\ \theta=0.5,$

at $X=1,\ \psi=\psi_X=0,\ \Omega=-\psi_{XX},\ \theta=-0.5,$

$Y=0,\ 1,\ \psi=\psi_Y=0,\ \Omega=-\psi_{YY},\ \dfrac{\partial\theta}{\partial Y}=0$

It is of interest to note that the boundary conditions for the vorticity transport equation (2.6) are not explicity known and have to be evaluated by using Eq. (2.5) at the walls. This is one of the well known difficulties that arise in the solution of the problem. With the spline technique however, ψ_{XX} and ψ_{YY} may be directly determined using the basic spline relations, a distinct advantage computationally.

III. Numerical Solution

In this study, the SADI (Spline-Alternating-Direction-Implicit) procedure was used to generate an algorithm resulting in a tridiagonal system containing either function values or first derivatives at the node points. The boundary conditions were evaluated using a general formula obtained from the basic spline formulae. The principal formulations are presented in Appendices

Vorticity equation

In the two-step procedure the algorithm obtained for the first step is:

$$\Omega^{n+1/2}_{i,j}=\Omega^{n}_{i,j}+\frac{\Delta\tau}{2}\Big[-(\psi^{n}_{Y}m^{n+1/2})_{i,j}+(\psi^{n}_{X}l^{n})_{i,j}$$

$$+\Pr\Big(M^{n+1/2}_{i,j}+L^{n}_{i,j}+\mathrm{Ra}\Pr g^{n+1}_{i,j}\Big)\Big]$$

$$=F_{i,j}+R_{i,j}m^{n+1/2}_{i,j}+Q_{i,j}M^{n+1/2}_{i,j} \tag{3.1}$$

where

$F_{i,j}$, $R_{i,j}$, $Q_{i,j}$ are known from the previous time step.

In the second step, the values of Ω are updated from time $(n+1/2)\Delta\tau$ to $(n+1)\Delta\tau$ as in standard ADI methods.

$$\Omega^{n+1}_{i,j}=\Omega^{n+1/2}_{i,j}+\frac{\Delta\tau}{2}\Big[-(\psi^{n}_{Y}m^{n+1/2})_{i,j}+(\psi^{n}_{X}l^{n})_{i,j}$$

$$+\Pr(M^{n+1/2}_{i,j}+L^{n+1}_{i,j}+\mathrm{Ra}\,g^{n+1}_{i,j})\Big]$$

$$=F'_{i,j}+R'_{i,j}l^{n+1}_{i,j}+Q'_{i,j}L^{n+1}_{i,j} \tag{3.2}$$

Where the following notation has been used

$$m=\partial\Omega/\partial X,\quad M=\partial^2\Omega/\partial X^2,\quad l=\partial\Omega/\partial Y,\quad L=\partial^2\Omega/\partial Y^2,\quad g=\partial\theta/\partial X$$

Eqs. (3.1) and (3.2) have been solved by using Eq. (A.2) in Appendix The values of Ω are evaluated directly with the boundary conditions

$$(\Omega^{n+1/2})_{X=0}=-(\psi^{n}{}_{XX})_{X=0};\quad (\Omega^{n+1/2})_{X=1}=-(\psi^{n}{}_{XX})_{X=1}$$

$$(\Omega^{n+1})_{Y=0}=-(\psi^{n}{}_{YY})_{Y=0};\quad (\Omega^{n+1})_{Y=1}=-(\psi_{YY})_{Y=1}$$

ψ_X, ψ_Y, ψ_{XX}, ψ_{YY} being obtained from the stream function equation at time $n\cdot\Delta\tau$.

In order to obtain the values of the first derivatives $m_{i,j}^{n+1/2}$, $l_{i,j}^{n+1}$ a tridiagonal formulation containing only first derivatives was used it being unnecessary to specify additional boundary conditions. $M_{i,j}^{n+\frac{1}{2}}$, $L_{i,j}^{n+1}$ were evaluated in a similar fashion.

Energy equation

For the first time step in the X direction, Eq. (A.2) from Appendix was used with the boundary conditions.

$$\theta_{X=0}=0.5, \qquad \theta_{X=1}=-0.5$$

$$\theta_{i,j}^{n+1/2}=\theta_{i,j}^{n}+\frac{\Delta\tau}{2}\Big(-(\psi_Y g^{n+1/2})_{i,j}+(\psi_X k)_{i,j}^{n}+G_{i,j}^{n+1/2}+K_{j,i}^{n}\Big)$$

$$=F_{i,j}+R_{i,j}g_{i,j}^{n+1/2}+Q_{i,j}G_{i,j}^{n+1/2} \tag{3.3a}$$

where

$$G=\frac{\partial^2\theta}{\partial X^2},\quad k=\frac{\partial\theta}{\partial Y},\quad K=\frac{\partial^2\theta}{\partial Y^2}$$

For the second time step

$$\theta_{i,j}^{n+1}=F''_{i,j}+R''_{i,j}k_{i,j}^{n+1}+Q''_{i,j}K_{i,j}^{n+1} \tag{3.3b}$$

The alternate equation (A.3) in the Appendix, which contains the first derivatives only, was used since the adiabatic wall condition implies zero first derivatives. i.e. $(k)_{Y=0}^{n+1}=(k)_{Y=1}^{n+1}=0$, then $\theta_{i,j}^{n+1}$ may be evaluated by a recursive relation with the following form (with the index i omitted)

$$\theta_j^{n+1}=\frac{d_j-a_j\theta_{j-1}^{n+1}}{b_j} \qquad j\neq 0$$

with

$$\theta_0^{n+1}=\frac{d_0b_1-d_1b_0}{a_0b_1-a_1b_0}$$

where

$$a_0=1+6Q_0''/h_1^2;\quad b_0=1-a_0$$

$$d_0=F_0''+R_0''k_0^{n+1}-Q_0''\left(\frac{2k_1^{n+1}+4k_0^{n+1}}{h_1}\right)$$

$$a_j=-6Q_j''/h_j^2;\qquad b_j=1-a_j$$

$$d_j=F_j''+R_j''k_j^{n+1}+Q_j''\left(\frac{2k_{j-1}^{n+1}+4k_j^{n+1}}{h_j}\right)$$

$$h_j=Y_j-Y_{j-1}\ \text{(grid spacing)}$$

Stream function equation

The stream function equation may be rewritten as a Cauchy-Kowaleska equation

$$\frac{\partial\psi}{\partial t}=\nabla^2\psi+\Omega$$

The first step in the solution procedure is

$$\psi_{i,j}^{n+1/2}=\psi_{i,j}^{n}+\frac{\Delta t}{2}(L_{i,j}^{n}+\Omega_{i,j}^{n})+\frac{\Delta t}{2}M_{i,j}^{n+1/2}=T_{i,j}+w_{i,j}M_{i,j}^{n+1/2} \tag{3.4}$$

while the second step results in

$$\psi_{j,i}^{n+1}=\psi_{i,j}^{n+1/2}+\frac{\Delta t}{2}(M_{i,j}^{n+1/2}+\Omega_{i,j}^{n})+\frac{\Delta t}{2}L_{i,j}^{n+1} \tag{3.5}$$

Equations (3.4) and (3.5) are solved in a similar manner to the second step of the Energy equation. No difficulties arise since the boundary conditions are appropriately specified. To obtain steady state solutions, repeated iterations until convergence are necessary. As the SADI procedure is unconditionally stable, large fictitious time steps may be used. Clearly, with this procedure, any intermediate results would not be representative of any time transient solution.

Nusselt number calculations

$$Nu(X)=-\frac{\partial\theta}{\partial X}+U\theta \tag{3.6}$$

$$\overline{Nu}(X)=\int_0^1 \mathrm{Nu}(X)dY \tag{3.7}$$

The first term in equation (3.6) represents the flux transport due to conduction, the second term is the contribution due to heat advection and increases with increasing Rayleigh Number. Theoretically, $\overline{Nu}(X)$ would be independant of X and equal to the values calculated on the vertical walls. Numerically, this property is generally not satisfied and the maximum difference between the $\overline{\mathrm{Nu}}(X)$ values may be used to check the accuracy of the numerical method.

IV. Results and Discussion

Transient flow

The computations were performed for the transient convective regime in a square cavity for values of $\mathrm{Ra}=10^7$ and 2×10^7 the Prandtl number being of the values from 0.71 to 10 (the condition $\mathrm{Ra}>\mathrm{Pr}^{16}$ imposes the value $\mathrm{Pr}=2.7$ as a limit value to access to regime VI). The initial conditions imposed were $U=V=\Omega=\theta=0$. In order to provide high resolution in the "boundary layer" region near the walls, a non uniform mesh was used with the spacing ratio from wall to centre-line $h_{i+1}/h_i=1.28$for the mesh which was 21 by 21 which being $h_{i+1}/h_i=1.18$ for 31×31. The time step $\Delta\tau=10^{-5}$ was used in the vorticity and energy equations while being $\Delta t=0.05$ for stream function equation.

The computations were carried out for the transient convective regime called VI by Patterson et al[1,2]. In a square cavity, the condition for this flow to exist is given by: $\mathrm{Ra}>\mathrm{Pr}^{16}$. Starting from a fluid at zero conditions, the evalution to steady state is divided into four transient sub-region with the following hierachy of reduced time scales and main features:

times scales		main features
$\tau_1=\mathrm{Ra}^{-0.5}$	(4.1)	Thermal boundary layer and inertial intrusions formed
$\tau_2=1/(\mathrm{Pr}^{1/3}\mathrm{Ra}^{5/12})$	(4.2)	Inertial intrusions reach the far end wall, internal wave activity and layering commence.
$\tau_3=\mathrm{Ra}^{-0.25}$	(4.3)	Cavity filled by horizontal layering but internal wave activity present.

$$\tau_\infty = \mathrm{R}\tau^{-1} \qquad (4.4)$$

Steady state by decay of wave motion. Distinct velocity and thermal layers present . The flow in dominated by inertia and the heat transfer by convection.

$$P = 2\pi\sqrt{2/\mathrm{Ra}\cdot\mathrm{Pr}} \qquad (4.5)$$

Period of internal wave motion.

The transient solutions are shown in the Fig. 1a – 1d for Ra = 10^7 and Pr = 0.71. The characteristics of the transient convective regime are very similar to those obtained by using the method of spline fractional steps. They will be presented in another paper [12].

In Fig. 2a, the transient temperature profiles in the horizontal middle plane are shown. Fig. 2b shows the vertical velocity profiles in the horizontal middle plane. At $\tau_0 = 10^{-4}$, the core may be regarded as stationary. As the time increases, the convective effects and the core activity become very strong. The dependence of the mean convective flux on τ is given in Fig. 2c. It is difined by:

$$q_{ov} = \int_0^1 U\theta dY$$

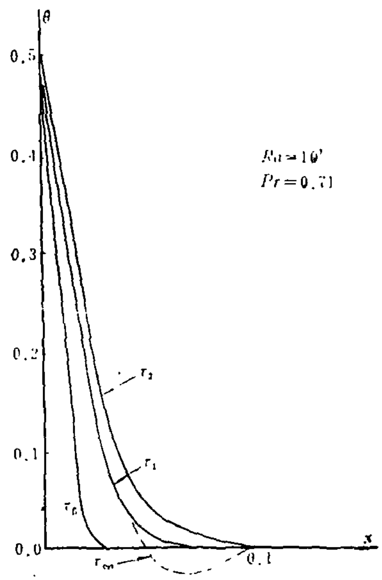

(a) Temperature distribution in the horizontal middle plane

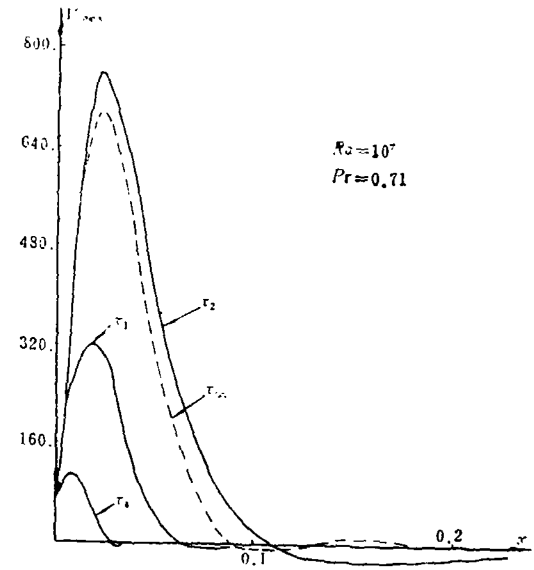

(b) Vertical velocity profile in the horizontal middle plane

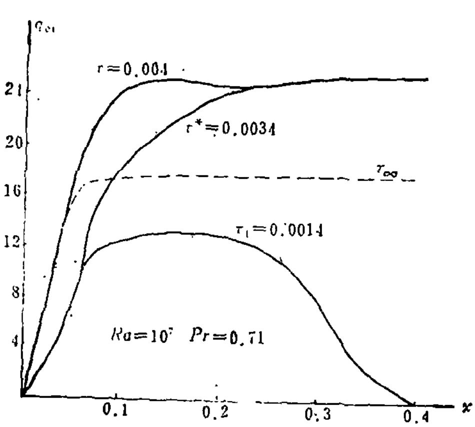

(c) Mean convective flux

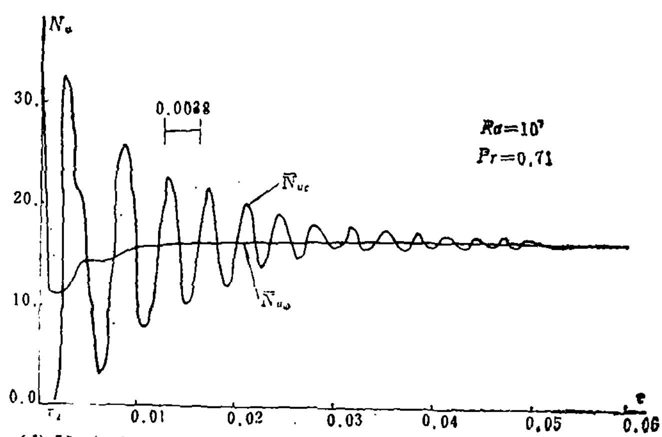

(d) Variations of the mean Nusselt numbers Nu_c and Nu_w as a function of time

Fig.2

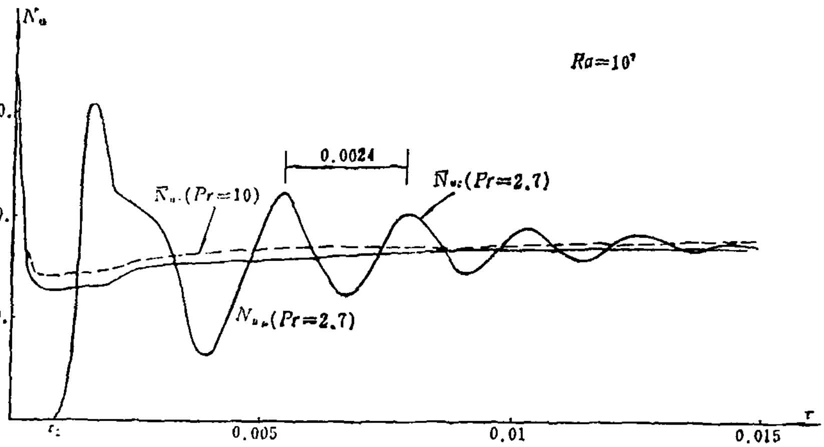

Fig. 3 Variations of the mean Nusselt number Nu_c as a function of time for different Prandtl numbers

The variations with τ of the Nusselt number at hot wall (Nu_w) and in the middle plane of the cavity (Nu_c) are shown in Fig. 2d. The τ_2 value is indicated and it appears that the scale analysis of [1,2] allows to properly predict the beginning of the internal wave motion. The period of the internal wave motion is given on the figure and its value is in good agreement with the theoretical predictions ($p=0.00334$).

The dependence of the oscillation of Nu_c on Pr is given in Fig. 3. The results show evidence together with Fig. 1d that, as the value of Prandtl number increases, the period of the internal wave

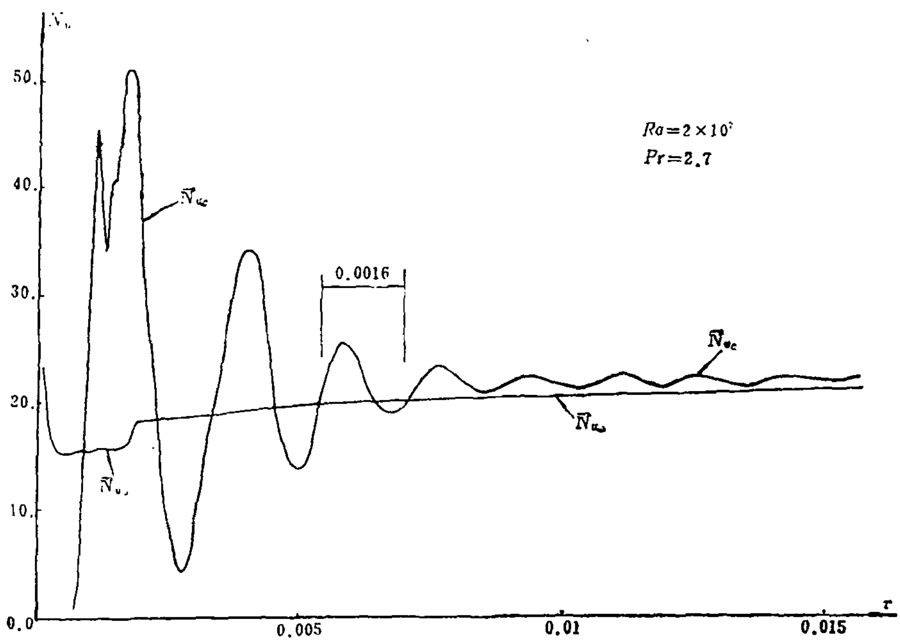

Fig. 4 Variations with t of Nusselt numbers for $Ra=2\times10^7$ and $Pr=2.7$

motion decreases with a ratio $p_2/p_1=(\mathrm{Pr}_1/\mathrm{Pr}_2)^{0.5}$. For Pr = 10, $\mathrm{Pr}^{16} \gg \mathrm{Pa}$, the oscillations of Nu_c doesn't arise. For Pr = 3.0, however, the transient convective regime is very similar to those obtained for Pr = 2.7, although in this case $\mathrm{Pr}^{16} > \mathrm{Ra}$. It seems that the condition $\mathrm{Pr}^{16} < \mathrm{Ra}$ is of scale signification only.

In Fig. 4, the variations with τ of Nusselt number for Ra = 2×10^7 and Pr = 2.7.

Table 1 Comparison of the steady state solutions at Ra = 10^7 and Pr = 0.71

Mesh size	ψ_c	V_{max}	U_{max}	Nu_w	Nu_c	Nu_{min}	Nu_{max}
31×31	29.48	710.27 X=0.0192	149.68 Y=0.873	16.73	16.68	1.425 Y=1	40.00 Y=0.0192
[12] 31×31	30.08	710.77 X=0.0192	150.16 Y=0.873	16.70	16.77	1.448 Y=1	39.00 Y=0.0192
[10] 31×31	29.08	697.28 X=0.0215	144.49 Y=0.860	16.66	16.34	1.387 Y=1	40.42 Y=0.017
Ref [13]	—	728.23 X=0.0237	147.56 Y=0.888	16.34	—	1.416 Y=1	36.50 Y=0.011

Table 2 The Steady State Solutions at Ra = 2×10^7 and Pr = 0.71

Mesh size	ψ_c	V_{max}	U_{max}	Nu_w	Nu_c	Nu_{min}	Nu_{max}
31 × 31	38.02	1051.20 x = 0.018	203.63 y = 0.879	20.08	20.87	1.906 y = 0.99	49.22 y = 0.018

The steady state results for Ra = 10^7 and Ra = 2×10^7 are reported in Table 1 and Table 2. The comparisons with available finite element data of Upson[13] from [10]) and the spline solution from [10] also given in Table 1 for Ra = 10^7 and Pr = 0.71. In the Tables, the symbols have the following significance: ψ_c -the stream function at the center of the cavity; U_{max} -the maximum horizontal velocity on the vertical middle plane. V_{max} -the maximum vertical velocity on the horizontal middle plane. The values of the minimum and maximum local Nusselt numbers on the hot wall together with their locations are shown also.

V. Conclusions

The numerical solutions of the transient convective flow at Ra = 10^7 and Ra = 2×10^7 have been obtained. The results are in good agreement with the theoretical predictions.

The SADI method seems to be an effective procedure for solving the problem of unsteady natural convection flow in square cavity at high Rayleigh numbers. The main advantages of using cubic spline approximation are that:

(1) The governing matrix system obtained is always tridiagonal.

(2) A variable mesh may be used without an introduction of a numerical viscosity since the truncation error is $O(h^3)$ on the first derivatives.

(3) Since the values of first or second derivatives may be evaluated directly, boundary conditions containing derivatives may be directly incorporated into the solution procedure thus avoiding the difficulty that exists with conventional finite difference schemes.

Acknowledgment The author wish to express his sincere thanks to the Computer Center of Lanzhou University for their effective support.

APPENDIX

In this section, the results of some simple developments are presented. (From Wang and Kahawita[8])

For example, after an equation of the type (3.1) has been obtained, it may be converted with the aid of the spline formulae into three useful forms containing exclusively either the function values, first derivatives or second derivatives.

Consider the following system of equations

$$u_i^{n+1}=F_i^{n+1}+R_i^{n+1}m_i^{n+1}+Q_i^{n+1}M_i^{n+1} \tag{A.1}$$

1) The transformed system containing function values only (and with the time index n + 1 omitted) may be written.

$$A_iu_{i-1}+B_iu_i+C_iu_{i+1}=D_i \qquad (i=1,\ N) \tag{A.2}$$

Where

$$A_i=\frac{e_ih_i}{6c_i}-\frac{1}{h_i}$$

$$B_i=\frac{d_ih_i}{6c_i}+\frac{e_{i+1}(h_i+h_{i+1})}{3c_{i+1}}-\frac{R_{i+1}(h^2_{i+1}+3R_ih_{i+1}-6Q_i)}{36c_{i+1}}+\frac{h_i+h_{i+1}}{h_ih_{i+1}}$$

$$C_i=\frac{d_{i+1}(h_i+h_{i+1})}{3c_{i+1}}-\frac{R_i(2h^2_{i+1}-3R_{i+1}h_{i+1})-6Q_i(h_{i+1})}{36c_{i+1}}-\frac{1}{h_{i+1}}$$

$$D_i=\frac{a_ih_i}{6c_i}+\frac{a_{i+1}(h_i+h_{i+1})}{3c_{i+1}}-\frac{F_{i+1}(2R_ih^2_{i+1}-6Q_ih_{i+i})+F_iR_{i+1}h^2_{i+1}}{36c_{i+1}}$$

and

$$a_i=\frac{F_iR_{i-1}h_i}{6}+F_{i-1}\left(\frac{R_ih_i}{3}+Q_i\right)$$

$$c_i=\frac{R_iR_{i-1}h^2_i}{36}-\frac{(R_ih_i+3Q_i)(R_{i-1}h_i-3Q_{i-1})}{9}$$

$$d_i=R_{i-1}\left(\frac{h_i}{6}-\frac{R_i}{2}-\frac{Q_i}{h_i}\right)$$

$$e_i=R_i\left(\frac{h_i}{3}+\frac{R_{i-1}}{2}\right)+Q_i\left(1+\frac{R_{i-1}}{h_i}\right)$$

$$h_i=x_i-x_{i-1}$$

2) The equations containing first derivative values only are

$$A_im_{i-1}+B_im_i+C_im_{i+1}=D_i \qquad (i=1,\ N) \tag{A.3}$$

Where

$$A_i=\frac{1}{3h_i}-\frac{2Q_i+4Q_{i-1}-R_{i-1}h_i}{h^3_i\Delta_i}$$

$$B_i=\frac{2}{3}\left(\frac{1}{h_i}+\frac{1}{h_{i+1}}\right)-\frac{2Q_{i+1}+4Q_i-R_ih_{i+1}}{h^3_{i+1}\Delta_{i+1}}-\frac{2Q_{i-1}+4Q_i+R_ih_i}{h^3_i\Delta_i}$$

$$C_i=\frac{1}{3h_{i+1}}-\frac{2Q_i+4Q_{i+1}+R_{i+1}h_{i+1}}{h^3_{i+1}\Delta_{i+1}}$$

$$D_i=\frac{F_{i+1}-F_i}{h^2_{i+1}\Delta_{i+1}}+\frac{F_i-F_{i-1}}{h^2_i\Delta_i}$$

$$\Delta_i=1+6\left(\frac{Q_i+Q_{i-1}}{h^2_i}\right)$$

3) The system with second derivatives only is

$$A_iM_{i-1}^{n+1}+B_iM_{i+1}^{n+1}+C_iM_{i+1}^{n+1}=D_i \qquad (i=1,\ N) \tag{A.4}$$

where

$$A_i=\frac{h_i}{6}+\frac{R_i+2R_{i-1}}{6\Delta_i}-\frac{Q_{i-1}}{h_i\Delta_i}$$

$$B_i=\frac{h_i+h_{i+1}}{3}-\frac{R_{i+1}+2R_i}{6\Delta_{i+1}}+\frac{2R_i+R_{i-1}}{6\Delta_i}+Q_i\left(\frac{1}{\Delta_{i+1}h_{i+1}}+\frac{1}{\Delta_ih_i}\right)$$

$$C_i=\frac{h_{i+1}}{6}-\frac{2R_{i+1}+R_i}{6\Delta_{i+1}}-\frac{Q_{i+1}}{h_{i+1}\Delta_{i+1}}$$

$$D_i=\frac{F_{i+1}-F_i}{\Delta_{i+1}h_{i+1}}-\frac{F_i-F_{i-1}}{\Delta_ih_i}$$

$$\Delta_i=1-\frac{R_i-R_{i-1}}{h_i}$$

References

[1] Patterson, J. and J. Imberger, unsteady natural convection in a rectangular cavity, *J. Fluid Mech.*, 100 (1980), 65 – 86.

[2] Patterson, J.C., On the existence of an oscillatory approach to steady natural convection in cavities, *ASME Journal of Heat Transfer,* 106 (1984), 104 – 108.

[3] Rubin, S.G. and R.A. Graves, Viscous flows solutions with a cubic spline approximation, *Computer and Fluids,* 3 (1975), 1 – 36.

[4] Rubin, S.G. and P.K. Khosla, Higher order numerical solutions using cubic splines, *AIAA JOurnal,* 14 (1976), 851 – 858.

[5] Wang, P. and R. Kahawita, Numerical integration of partial differential equations using cubic splines, *Int. J. Computer Math.,* 13 (1983), 271 – 286.

[6] Wang, P. and R. Kahawita, The numerical solution of burgers equation using splines, *Acta Aerodynamica Sinica,* 2 (1984), 11 – 18.

[7] Wang, P., Spline-Lax-Wendroff scheme.and spline-leap-frog scheme, *Acta Aerodynamica Sinica,* 3 (1985), 90 – 96. (in Chinese)

[8] Wang, P. and R. Kahawita, A two-dimensional model of estuarine circulation using cubic splines, *Can. J. Civil Eng.,* 10 (1983), 116 – 124.

[9] De Vahl Davis, G., Natural convection of air, a square cavity: an accurate numerical solution, *Report FMT*/1, University of N.S.W., Kensington, Australia (1981).

[10] Lauriat, G., Accurate solutions of natural convection flow in square cavities at high raleigh numbers with a cubic spline approximation, *ASME* Winter Annual Meeting, Phoenix, Arizona (1982).

[11] Wang, P. and R. Kahawita, The numerical solution of the natural convection flow in a square cavity, *Proc. of 4th Int. Conf. on Mathematical Modelling in Science and Technology,* Zurich, Aug. 24 – 26 (1983, 640 – 645.

[12] Wang, P., Spline simulations of unsteady natural convection flow in a square cavity at Ra = 10^7 with method of fractional steps. (to appear in *Acta Mechanica Sinica*).

[13] Upson, C.D., P.M. Greho, and R.L. Lee, Finite element simulations of thermally induced convection in anenclosed cavity, *Report UCID* 18602, Lawrence Livermore Laboratory, Mars (1980).